

Article

Conceptual Design, Flying, and Handling Qualities Assessment of a Blended Wing Body (BWB) Aircraft by Using an Engineering Flight Simulator

Clayton Humphreys-Jennings, Ilias Lappas*, and Dragos Mihai Sovar

Department of Aeronautical and Mechanical Engineering, School of Engineering, University of South Wales, Treforest Campus, Treforest CF37 1DL, UK; 15068315@students.southwales.ac.uk (C.H.-J.); 14033550@students.southwales.ac.uk (D.M.S.)

* Correspondence: ilias.lappas@southwales.ac.uk; Tel.: +44-01443-482565

Received: 19 February 2020; Accepted: 26 April 2020; Published: 28 April 2020

Abstract: The Blended Wing Body (BWB) configuration is considered to have the potential of providing significant advantages when compared to conventional aircraft designs. At the same time, numerous studies have reported that technical challenges exist in many areas of its design, including stability and control. This study aims to create a novel BWB design to test its flying and handling qualities using an engineering flight simulator and as such, to identify potential design solutions which will enhance its controllability and manoeuvrability characteristics. This aircraft is aimed toward the commercial sector with a range of 3,000 nautical miles, carrying 200 passengers. The BWB design was flight tested at an engineering flight simulator to first determine its static stability through a standard commercial mission profile, and then to determine its dynamic stability characteristics through standard dynamic modes. Its flying qualities suggested its stability with a static margin of 8.652% of the mean aerodynamic chord (MAC) and consistent response from the pilot input. In addition, the aircraft achieved a maximum lift-to-drag ratio of 28.1; a maximum range of 4,581 nautical miles; zero-lift drag of 0.005; while meeting all the requirements of the dynamic modes.

Keywords: Blended Wing Body (BWB); aircraft conceptual design; engineering flight simulator; flying and handling qualities; aircraft stability

1. Introduction

The Blended Wing Body (BWB) aircraft is a non-conventional design in which the fuselage and the wings are combined into one fluid shape instead of three distinct parts assembled. This has the potential of providing various advantages “including a 15% reduction in take-off weight and a 27% reduction in fuel burn per seat mile” [1]. The reduction in fuel comes from the 15% increase in lift-to-drag ratio meaning less work needs to be done to overcome the effects of drag, but also, the design itself significantly reduces the amount of zero-lift, or parasite, drag that the aircraft is affected by [2,3].

This design follows very similar characteristics to that of the ‘flying wing’, including the downside that, without a horizontal stabilizer, the aircraft is liable to longitudinal and lateral instabilities, which is a phenomenon that has been reported for various prototypes and studies [4]. For the longitudinal stability, the short period mode exhibits shorter periods and less damping than conventional configurations. The phugoid mode is less damped than conventional aircraft as well [5]. With regards to the lateral stability, the main issue is to balance the yaw during roll manoeuvres, since in the BWB configuration the vertical control surfaces are reduced or absent. Work by Rahman and Whidborne [6] has shown that a feedback loop is needed for enhanced lateral stability due to the

oscillation and the damping factor of the Dutch roll mode. Apart from the potential flying and handling qualities issues, the BWB concept is also challenged with regards to its weight efficiency [7]. In theory, flying wings can be designed to be inherently stable [8] and there have been 'flying wings' that have flown successfully; an example of this being the Northrop YB-49. To be able to study the unique performance and stability characteristics of the BWB and the associated technical challenges from a performance, flying, and handling qualities point of view, a conceptual BWB design has been created that offers similar performance to a standard commercial aircraft design.

There are many research programs that have developed suitable BWB design outcomes on paper; however, these have not been tested on a large scale, simulator, or at all. Those efforts have been supported by NASA, Boeing, and multiple universities across Europe and USA and each of these initiatives has provided promising results with suggestions for future research to improve upon which will be inferred throughout the present study.

The multidisciplinary optimization of a BWB (MOB) was a joint European venture which has engaged 15 different universities with the intent to create a Computation Design Engine (CDE) following both a low and high fidelity multidisciplinary design process directed at a BWB design with their key objective to "create a system allowing both co-operative and innovative design to be undertaken by a distributed design team employing their own specific design tools and methods" [9]. Although their focus was more on developing a system that can be used to effectively optimize an array of unique and innovative designs for aircraft, the results from the testing of the CDE yielded interesting results that have been implemented into the present design such as "controllability can be improved by shortening the fuselage" and "increasing the aft-camber of the fuselage profiles". The aerodynamic considerations of the MOB platform [10] have also been taken into account at the present study, including the use of winglet rudders.

Liebeck [1] focused on exploiting the size and efficiency potential of the BWB aircraft, opting to create a design for 800 passengers and 7,000 nautical mile range in a double decker, double aisle design. The proposed design was compared to a conventional aircraft with the same capabilities utilizing multidisciplinary design optimization. His results were achieved through computational testing using standard equations which demonstrated a "15% reduction in take-off weight and a 27% reduction in fuel burn per seat mile", as well as the BWB being "readily adaptable to cruise Mach numbers as high as 0.95". This comes at very little extra cost in terms of manufacturing with many advantageous opportunities relating to environmental efficiency. Finally, the estimated maximum lift-to-drag ratio (L/D) ratio at cruise is 23 at a great reduction in thrust requirements, using only three engines at 61,600lbf as compared to a standard design achieving a maximum L/D of 19 and requiring four 63,600lbf engines. Trailing edge devices and winglet rudders have been used to perform various functions such as basic trim, control, pitch stability augmentation, and wing load alleviation.

Work of Van Dommelen and Vos [11] has attempted to create a systematic algorithm that will enable multidisciplinary optimization, to which they have ultimately investigated three different and unique design prospects explicitly for the BWB. These three design options are two backward swept wing designs with the engines first mounted under the wing, and then at the trailing edge of the fuselage; and one forward swept wing also with engines under-the-wing mounted. Their results were inconclusive as to which is best of the three with each demonstrating solutions to each problem: the forward swept wings meant that the static margin was greatly improved and even had the best ferry range; the forward sweep with under-the-wing engines had the least travelled static margin from take-off to cruise which is crucial for stability overall and had maximum lift coefficient; whilst the forward swept aft-mounted engines had the least fuel consumption and highest maximum L/D at 27.9. Another advantage of aft-mounted engines is that of reduced noise pollution which has become an increasingly important goal of city-based airports.

The X-48B Low Speed Vehicle (LSV) is an 8.5%-scale aircraft of a potential, full-scale BWB type aircraft and is flown remotely from a ground control station using a computerized flight control system located onboard the aircraft, which had the main purpose of looking into the stability of the BWB aircraft [12]. Thirty-nine flights were performed in various configurations which accumulated just under 22 hours of flight time, all with positive feedback from the pilot. The most important

outcome of this work is that the BWB can be controlled by a pilot without inducing errors and that the scaled design has been flight tested to meet a standard commercial flight envelope as well as further expansion of what the aircraft can handle.

2. Methodology

2.1. Geometry

2.1.1. Weights

Several studies have addressed the topic of developing a high capacity BWB design [1,2,13]. However, following relevant market research [14,15], it has been determined that the present study will attempt to provide a solution to the increasing future demand for a single aisle passenger aircraft. A BWB design of similar passenger capacity has been developed to compare its performance against an equivalent conventional Airbus A320 aircraft [16]. The design of the present study is set to achieve a range of 3,000 nautical miles and to carry a payload weight of 20,000 Kg or 200 people plus baggage. A typical mission profile for a passenger aircraft has been assumed ((Taxi, Warm Up → Take off → Climb → Cruise → Loiter → Descend → Landing and Taxi) and the weights have been calculated using a combination of methods. Mariens [17] and Roskam [18] methodologies have been used for the estimation of the fuel required for the baseline mission profile. Those methodologies use the Breguet performance theory together with statistical factors which estimate the fuel weight of each segment of the mission. Table 1 shows the values of the fuel fractions for each segment of a typical mission.

Table 1. Fuel fraction for each segment of a typical flight mission (modified using Roskam [18] as baseline).

| Flight segment | Fuel weight fraction (M_{ffi}) |
|--------------------------------------|------------------------------------|
| Start up and check list checks | 0.990 |
| Ground run and taxiing | 0.990 |
| Taking off and climbing | 0.975 |
| Cruising | Calculated |
| Descend, landing, taxi, and shutdown | 0.982 |

The fuel weight fraction M_{ffi} is defined as the ratio of the total aircraft weight at the end of the flight segment to the total weight of the aircraft when the segment has begun. Thus, the total fuel weight fraction defines the burned fuel as a ratio of the total aircraft weight at the end of the mission to the total aircraft weight at the beginning of the mission. As such, the total fuel weight fraction can also be expressed analytically as the product of all the fuel weight fractions, as per Equation (1)

$$M_{ff} = \prod_{i=1}^n M_{ffi} = 1 - \frac{W_{fuel}}{W_{take\ off}} \quad (1)$$

Initial weight approximations have been calculated using empirical relations from Raymer [19]. The approximations were then refined once again after the basic geometry was established and then iterated to converge. By estimating the maximum take off weight (MTOW) and the maximum zero fuel weight (MZFW), the weight of the aircraft at cruise W_{cruise} , was estimated by Equation (2) [20]

$$W_{cruise} = \sqrt{(MTOW) \times (MZFW)} \quad (2)$$

The final weight estimates are defined in Table 2, which also compares the weight estimates of the model with the weight data of the baseline version of the Boeing 737-800 aircraft [21].

Table 2. Final weight estimates

| | Weight (Kg) | Weight fraction | Boeing 737-800 Weight (Kg) (from [21]) | Boeing 737-800 Weight fraction | Percentage difference |
|------------------|--------------------|------------------------|---|---------------------------------------|------------------------------|
| Empty Weight | 39,523 | 0.491 | 41,500 | 0.525 | +5.00 |
| Fuel Weight | 20,869 | 0.259 | 20,894 | 0.265 (max. fuel) | +0.12 |
| Payload | 20,000 | 0.250 | 16,606 | 0.210 | -16.97 |
| MTOW | 80,392 | 1.000 | 79,000 | 1.000 | -1.73 |
| MZFW | 59,523 | 0.740 | 58,106 | 0.735 | -2.38 |
| Weight at cruise | 69,175 | 0.860 | 67,752 | 0.858 | -2.05 |

A sizing methodology for the conceptual design of BWB transports has been suggested by Bradley [22]. His study compares, among others, weight estimates of BWB designs having 250 to 450 passengers with weights of similarly sized conventional passenger aircraft. It has been observed that the weight trends among the BWB configurations show a similar pattern to the conventional transports. The BWB of the present study offers an enhanced payload capacity when compared to the similarly sized (similar MTOW) Boeing 737-800.

2.1.2. Wings

Once the weights were determined, the wing geometry was able to be defined; this was calculated for the main wing section using the Boeing 787-800's Aspect Ratio (AR) of 9.44 [23] as an initial reference value. In addition, the sweep of the outboard wing was determined to be 40 degrees, while the sweep of the inboard wing as 58 degrees. This was chosen since it provides the highest lift-to-drag ratio for a slight negative moment generated at the wings [24,25]. The design of the wings has adopted best practices of previously published BWB studies [1,9,10,16,22] with values for certain wing design parameters (taper ratio for example) that have been based on their potential for achieving a wing that is as efficient as is practicable. The best practices show that the wing area of a BWB should normally be a multiple of the wing area of a conventional passenger aircraft having a similar MTOW. This leads to lower wing loading (W/S) values for the BWB designs and as such, from a performance point of view, the potential of the BWBs to achieve high values of maximum speed is limited. Instead, it offers flexibility in terms of sizing the flaps of the wing, as the lower W/S values incur lower stall speeds than the conventional configurations. This has been evident for the BWB design at the performed flight test. With regards to the AR value, various ideas and approaches have been explored and tested in conjunction with the decision for the most suitable sweep angles. The benefit of using the engineering flight simulator has enabled the testing of various embryonic wing shapes with different parameters at the early stages of the development. Thus, the wing configuration has been finalized by using performance, handling and stability criteria, in line with the objectives of the study. The benefits of the sweep angle to both the directional and lateral stability of the platform, as well as to the relative position of the aerodynamic center with respect to the center of gravity (CG) and to delaying the transition to transonic speeds have been prioritized, resulting in an AR value of 4.25, while the wingspan was kept close to the value of the Boeing 737-800.

The tendency of the BWB aircraft is to pitch up due to the position of the aerodynamic center typically being in front of the CG, and no horizontal stabilizer or tail to counteract it [26]. This can be counteracted using mass positioning but also negative moments. Having taken into account all those considerations, Table 3 outlines the results for the wing geometry.

Table 3. Wing geometry

| Parameter (unit) | Value |
|---|--------|
| Span, b (m) | 36.81 |
| Area, S (m ²) | 318.81 |
| AR | 4.25 |
| Taper ratio, λ | 0.225 |
| Root chord length, c_{root} (m) | 6.34 |
| Tip chord length, c_{tip} (m) | 1.43 |
| Mean aerodynamic chord, MAC (m) | 4.40 |
| MAC distance from center line, Ψ (m) | 7.26 |

Rudder winglets have been used for adequate yaw control as a design feature which has been tested at previous BWB passenger aircraft studies [1,10]. Post flight test simulation analysis has resulted in changing the geometry of the rudder winglets initially used to aid in directional control. An initial reference value of 20% of the semispan [27] of the wing of the BWB had been taken at the early development stage for the span of the winglet rudder. This was a value of 3.68 m which had to be increased, due to not being adequately reactive with pilot input. Following the feedback received by the test pilot during the execution of the dynamic stability modes, the span has been finalized to 4.5 m, with a chord length of 0.45 m. The literature shows that rudder winglets have been also used at smaller sized platforms, providing not only yaw but pitch control as well [28].

The chosen aerofoil for the inner wing and fin was the supercritical NACA sc0012 as this has been proved to be the most appropriate for the flying and handling qualities for the BWB design during the flight test simulations. Non-symmetric aerofoils like the supercritical NACA sc2412 have been tested as well. However, that aerofoil was used for the outer wing based on its efficiency and on the fact that it has the same thickness-to-chord ratio as the one used for the inner wing. From the data created by XFLR5 (v6.47), shown in Figure 1, it is observed that the aircraft is stable straight off with a negative gradient for the moment coefficient c_m . The neutral point was determined to be at 13.41 m from the nose, and the CG at 12.34 m. This meant a static margin of 8.65% of the MAC, meaning that it is stable, and above the recommended 5% static margin.

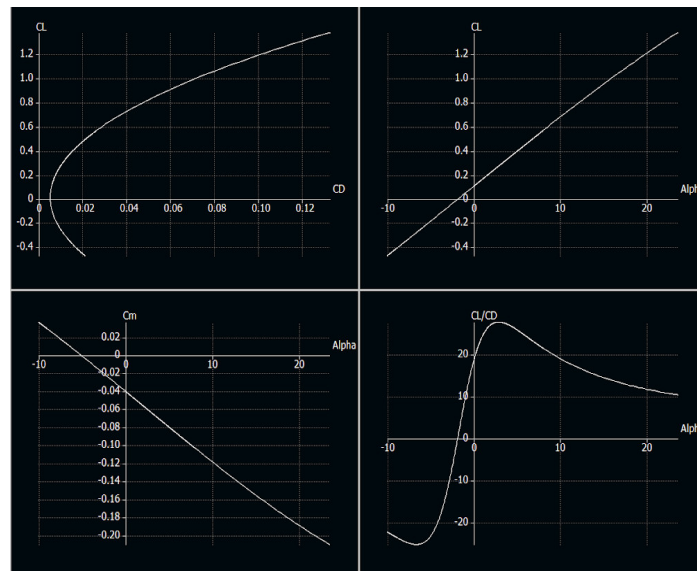


Figure 1. XFLR5 (v6.47) Results. Top-left: C_L vs C_D . Top-right: C_L vs angle of attack. Bottom-left: C_m vs angle of attack. Bottom-right: C_L/C_D vs angle of attack.

Further development of the wing has been undertaken to enable a more efficient design and the effort has yielded positive outcomes with regards to the flying and handling characteristics of the BWB design. As a first step in reshaping the wing geometry, the main approach that has been

considered was imprinting the elliptical lift distribution, which results in the lowest induced drag for a given span [29]. To achieve the specified distribution, the overall geometry of the BWB design has been incorporated to the OpenVSP (v3.17.0), which employs the vortex lattice method (VLM). The methodology implies the variance of four different twist values at different spanwise positions. Figure 2 shows the twist values along the wing. Comparatively, Qin et al. [30], have determined using a low fidelity panel method combined with high fidelity RANS approach that, among other findings, a twisted wing with a mix of triangular and elliptical distribution is best as a compromise between least wave drag for the triangular and the lowest induced drag for the elliptical distribution.

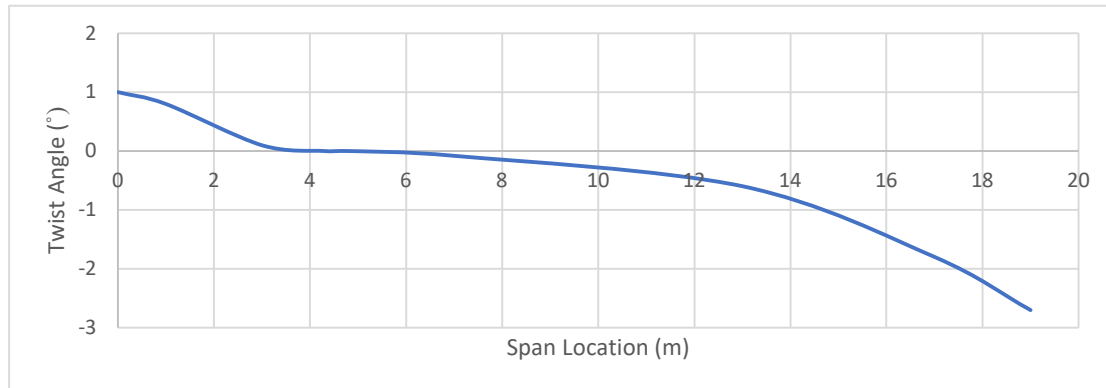


Figure 2. Spanwise twist distribution of the re-shaped wing model.

The resulting drag coefficient reduction is presented at the Table 4.

Table 4. Drag coefficient reduction following wing re-shaping

| | Induced drag coefficient ($C_{D,i}$) | Zero lift drag coefficient ($C_{D,0}$) | $C_{D(total)}$ |
|-------------|--|--|----------------------------------|
| Non-twisted | 0.0089 | 0.0046 | 0.0135 |
| Twisted | 0.0086 | 0.0045 | 0.0131 |
| Difference | -3.49% | -2.81% | -3.26% |

The sectional lift coefficient required for the elliptical lift distribution follows a steadily increasing trend from the centerline section plane of the BWB design until the beginning of the wing, as shown in Figure 3. A more visible increment is noticed from the beginning of the wing until a maximum is reached at approximately its middle section. Then, a steep decrease is noticed until the beginning of the winglets.

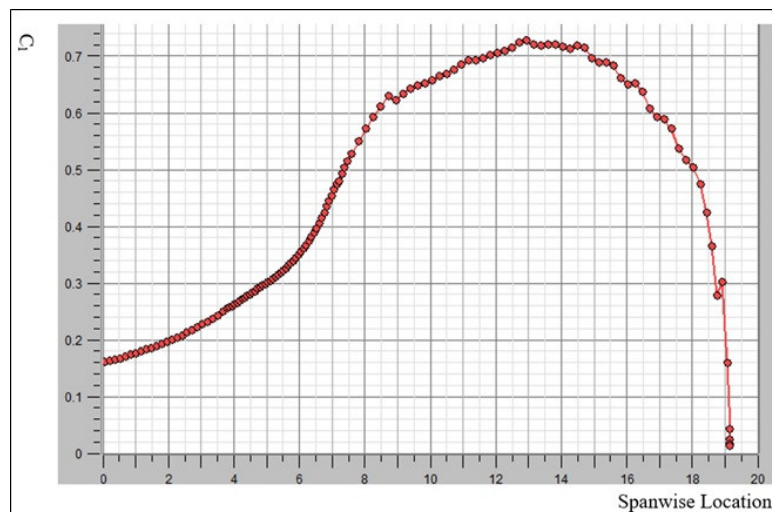


Figure 3. Local lift coefficient distribution across the wingspan.

Kumar and Khalid [31] have used the same trend of the sectional lift coefficient for a similar BWB concept. However, the method used in the present study for obtaining the twist angles is based on the lift curves. Using a low fidelity panel method, Qin et al. [10,30,32] have managed to achieve an elliptical lift distribution and the present study has benefited from their method to achieve a similar distribution following the re-shaping of the BWB wing, as shown at Figure 4.

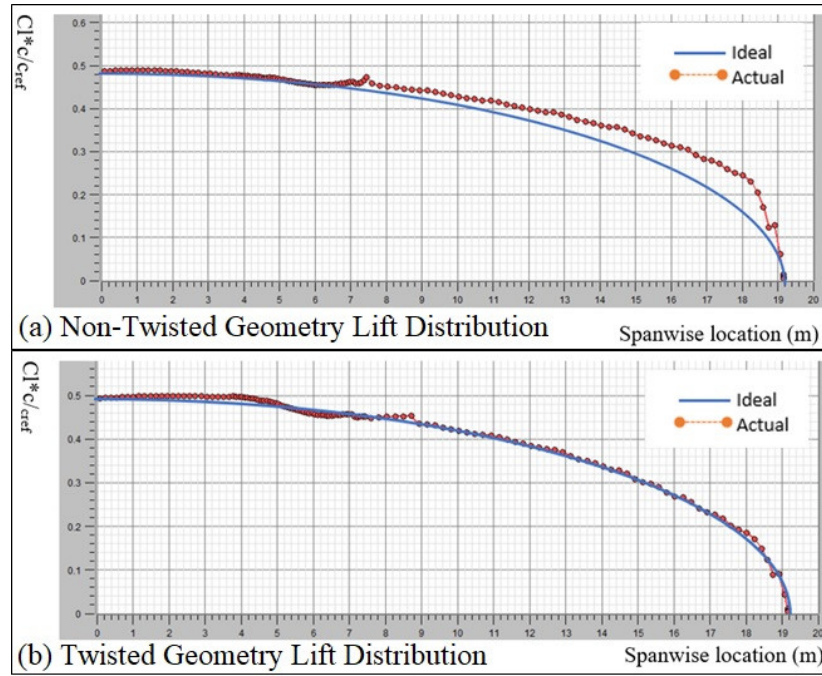


Figure 4. Spanwise lift distribution at cruise conditions.

As a further step when exploring a more robust optimization method of their designs, they have employed a high-fidelity RANS approach and this is also recommended by related studies of Panagiotou et al. [28] and Da Ronch et al. [33]. Various views of the re-shaped configuration are shown at Figure 5.



Figure 5. Various views of the re-shaped configuration.

2.2. Design Parameters Overview and Comparison

Table 5 below compares design parameters of the BWB aircraft of the present study (CHJ-BWB) against the conceptualized design of Ammar et al. [16], which is based on an Airbus A320 baseline, and of the Boeing 737-800 [21].

Table 5. Comparison of the conceptual design data

| Parameter (unit) | CHJ-BWB | Ammar et al. [16] | Boeing 737-800 [21] |
|---------------------------------------|---------|-------------------|---------------------|
| Wing area, S (m ²) | 318.81 | 367.8 | 124.48 |
| Wing span, b (m) | 36.81 | 56 | 34.32 |
| AR | 4.25 | 8.53 | 9.45 |
| Wing loading, W/S (N/m ²) | 2469.22 | 1969 | 6158.42 |
| Length, (m) | 30.74 | unknown | 39.50 |
| MTOW (Kg) | 80,392 | 73,828 | 79,000 |
| OEW (Kg) | 39,523 | 40,043 | 41,500 |

| | | | |
|--|--------|--------------------------|---------|
| Payload (Kg) | 20,000 | 20,000 (same pax number) | 16,606 |
| Fuel weight (Kg) | 20,869 | 13,785 | 20,894 |
| Range (nmi) | 4581 | 2354 | 3750 |
| Fuel weight required (Kg) per nmi per 1000 | 0.2278 | 0.2928 | 0.3355 |
| Kg payload (1/nmi) | | | |
| L/D maximum | 28.1 | 22.17 | 17.26 |
| CG (% MAC) | 8.652 | unknown | unknown |
| Take off distance (Km) | 3.12 | 1.38 | 2.50 |
| Landing distance (Km) | 1.30 | unknown | 1.77 |
| Stall speed-clean configuration (KIAS) | 130 | unknown | 128 |

The comparison illustrates the performance advantages of BWB designs when compared to conventional passenger aircraft designs. The BWB designs offer considerably lower values for the fuel required per nautical mile to carry one metric ton of payload and this is mainly attributed to their ability of achieving considerably higher maximum L/D values than the conventional designs. Another observed trend is that for similarly sized platforms (similar MTOW), the BWB designs will require more than twice the wing area required by the conventional passenger aircraft and this influences the typical wing loading values observed at BWB platforms.

3. Engineering Flight Simulator Set Up and Flight Testing

Once the BWB design has been finalized, its parameters have been inserted into the Merlin MP521 Engineering Flight Simulator [34], to test its flying and handling qualities. The MP521 simulator comprises a capsule with a six-axis motion system, visual and instrument displays, touch control panels, and hardware flight controls. The software of the engineering flight simulator that has been run is the Excalibur II, while the design has been created at the Excalibur Data Editor. The model in the editor has utilized the geometric data and mass properties of the design, in addition to the aerodynamics and propulsion data, acquired during the BWB conceptual design. The mass moments of inertia are calculated by the data editor, using empirical relations, from the inserted values that correspond to the aircraft mass parameters, CG, and wing span, assuming one plane of symmetry.

Figure 6 shows the Merlin MP521 engineering flight simulator capsule, Figure 7 its instructor station, and Figure 8 the head up display of its main console. In flight data parameters can be recorded with frequencies of up to 25 Hz, to be used for post flight review and analysis.



Figure 6. Engineering flight simulator capsule



Figure 7. Engineering flight simulator instructor station

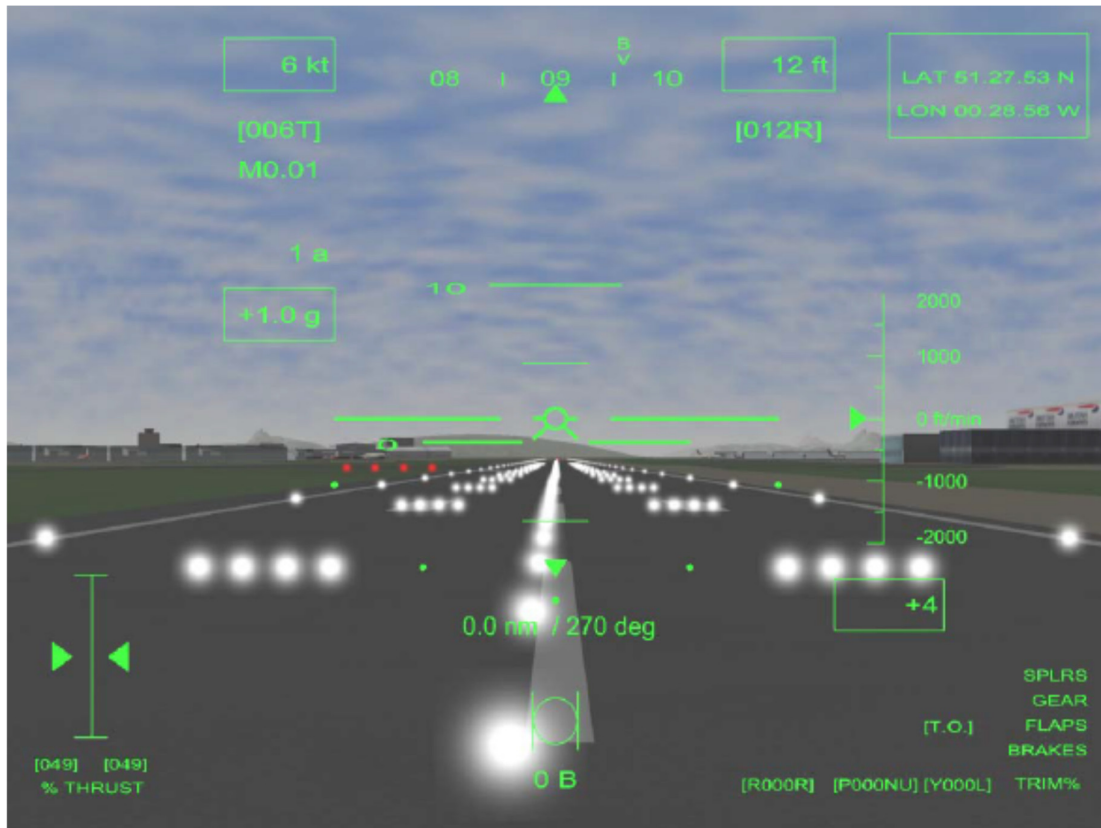


Figure 8. Engineering flight simulator main console head up display showing flight parameters (from [35], copyright to Merlin Flight Simulation Group).

The Excalibur software does not recognize wing, tailplane, and fin design features, it instead requires conceptual design input in terms of horizontal and vertical panels. A wing, for example, is considered a horizontal surface and as such is modeled using the horizontal panels pages of the data editor. All elements at Excalibur are positioned with respect to the $X/Y/Z$ datums, including the undercarriage. Using Excalibur is not just the process of conceptual design data entry, it is also the understanding of what that conceptual design data is doing when the aircraft model is test flown so that the aircraft designer can 'tune (adjust)' the data to resolve anomalies in the performance of the model when dynamic testing is performed. An overview of the flight model editor is shown at the Figure 9.

The screenshot shows the 'Flight Model Editor' software interface, specifically the 'CG & Mass Parameters' page. The interface is divided into several sections:

- Aircraft Mass:** Includes input fields for Empty Mass (490 kg), Empty CG x (-0.5 m), Empty CG y (0.0 m), and Empty CG z (-0.33 m).
- Fuel:** Includes input fields for Fuel Capacity (86 kg), x Location (0.0 m), y Location (0.0 m), and z Location (0.0 m).
- Pilot Eye Position:** Includes input fields for x (-0.616 m), y (0.3 m), and z (-1.8 m).
- Aircraft Empty Inertia:** Includes a checkbox for 'Use computed values' and input fields for Zero Fuel inertia: Ixx (1413 kg.m²), Iyy (739 kg.m²), Izz (2171 kg.m²), Ixz (217 kg.m²), and Wing Span (10.3 m).
- Payloads:** A table with 5 columns and rows for Initial/Final Mass, Initial/Final x, y, z, Deploy Time, and Reload Time. All values are currently set to 0.0 or 10.0.
- Aircraft Axes:** A diagram showing the X (positive FORWARD), Y (positive RIGHT), and Z (positive DOWN) axes.
- Warning:** A red text box stating 'Do Not Leave Any Boxes Blank!'.
- Buttons:** An 'Apply' button is located at the bottom right.

Figure 9. Overview of the flight model editor (CG & Mass Parameters page, from [35], copyright to Merlin Flight Simulation Group).

To illustrate the conceptual design data entry process, the 'CG & Mass Parameters' page is selected at the Figure 9 above. It contains all the conceptual design information required for the mass, inertia and any payloads. The fuel is itemized separately because the fuel mass is taken and depleted in accordance with the specific fuel consumption of the specified propulsion system at the 'Propulsion' page. The aircraft mass, CG and inertia are calculated by the designer and entered on the page. The fuel capacity and position are both single entries which are representative of the combined masses and positions of the however many fuel cells of the conceptual design. The payloads require multiple entries of mass and positional data and payloads are defined as anything that is disposable from the aircraft (passengers, freight, and military stores among others). The Excalibur software calculates the final CG, mass, and inertia for the total aircraft and displays this information to the designer. Upon completion of the 'CG & Mass Parameters' page, the designer moves to the 'Fuselage' page and continues until all the required data entries of all the different pages (AirBrake, Propulsion, Undercarriage, etc.) of the flight model editor are completed.

The performed simulated flights followed a traditional commercial flight test path which included the static and dynamic modes [36]. A secondary objective of the flight test was to qualify the design to enter the 'IT FLIES UK' aircraft design, flying, and handling qualities international competition. This has required specific flight test documents to be completed that helped outline the parameters which had to be monitored when performing the initial flight tests of the aircraft. The rest of the flight tests have focused on checking compliance to the MIL-F-8785C requirements [37], as they have distinct pass/fail criteria with qualitative values with which to compare against, while looking at the dynamic modes at the various flight phases. These are divided into three categories, namely A (rapid maneuvering, e.g. air-to-air combat), B (gradual maneuvering without precision tracking, e.g., climb and cruise), and C (gradual maneuvering with precision tracking, e.g., take-off and landing). For the aircraft, it is intended to satisfy both B and C since it does not perform rapid maneuvers. Finally, levels of flying quality are labeled from 1 to 3, with 1 being the best and 3 being the worst. This design will be aiming for Level 1 where the aircraft's "Flying qualities clearly adequate for the mission flight phase" because this is meant for commercial aircraft and pilot load is already high without additional input required as in Level 2.

The time to double or half is the time required for the initial perturbation of the trimmed condition to be doubled or halved and is defined at the Equation (3).

$$t_{double} \text{ or } t_{half} = \frac{\ln 2}{|n|} = \frac{\ln 2}{|\zeta| \omega_n} \quad (3)$$

in which the symbol n corresponds to the real part of the relevant eigenvalue. The damping ratio ζ is defined by using the Equation (4).

$$\zeta = -\frac{n}{\omega_n} \quad (4)$$

in which ω_n is the undamped angular frequency provided by Etkin and Reid [38] at the Equation (5) below.

$$\omega_n = (\omega^2 + n^2)^{0.5} \quad (5)$$

thus, by obtaining the period (T) of the oscillation and the t_{half} or t_{double} after processing the recorded flight data, both the damping ratio and the undamped angular frequency have been calculated.

4. Results and Discussion

4.1. Flying and Handling Qualities

4.1.1. Take Off and Initial Climb

The design was initially able to take-off with MTOW at 170 KIAS with flaps at the take-off position in mean sea level ISA conditions and this required a distance of 2.46 Km; the time for which was 46 seconds. That meant that the speed for take-off was 1.79 times the stall speed observed during the flight simulations, whereas an accepted rule of thumb is that the take-off speed should be 1.1-times the stall speed. This suggests that the aircraft has had considerably more drag in the take-off configuration than clean, which has increased the value of the speed required before a successful take-off. On testing with a test pilot as part of the 'IT FLIES UK' competition, he has commented that the speed was relatively fast for a take-off and he has suggested if the aircraft can have a slightly more extended take-off flap setting, something which has been incorporated successfully into the final design and reduced the take-off speed to 150 KIAS, a value which compares satisfactorily to aircraft with similar MTOW.

4.1.2. Stall and Landing

The stall speed for the aircraft was recorded at 95 KIAS with fully extended flaps and 130 KIAS in clean configuration. Both did not demonstrate a standard nose down stall, but instead displayed nose 'nodding' which was commented on by the test pilot in positive regards. According to Nicolai and Carichner [39], the approach speed (with approach flaps setting) needs to be at least 1.3 times the stall speed, which for our aircraft would be at least 123.5 KIAS. From the data, it was determined that the average rate of descent for the aircraft in landing configuration was 817 ft/min which was achieved at an average speed of 151 KIAS with the pilot commenting that speed control was satisfactory. With the approach speed averaging at 151 KIAS, this has provided us with a nearly 1.6 times the stall speed safety margin. Additional testing did indicate that the aircraft would recover on its own if wing drop was induced by the pilot during the stall at various cruising altitudes, but, in general, no wing drop has been observed during a standard stall with wings level. During the landing, pitch control was sensitive with the pilot having no difficulty to fix an appropriate pitch attitude for landing.

4.1.3. Cruise and Trim Authority

Cruising conditions were met as part of the specification. The aircraft was able to fly at 35,000 ft at a maximum speed of 0.85 Mach and performed as expected. The test pilot noted a good overall roll performance and suitable for the mission requirements. During steady cruising conditions, the

trimmed aircraft did hold its own without any additional pilot input, which suggests that the static stability is adequate for non-dynamic modes. With regards to the trim authority set up for the simulation, the trim rate (percentage of total travel of the trim control surface per second) for a particular surface is very dependent upon the type of the aircraft. The trim rates used in the engineering flight simulator for pitch, roll, and yaw can be adjusted, either in isolation or together with any change in the geometry of the related control surface. The designer can experiment during the development of the design at the Flight Model Editor (Figure 9) using a high trim rate initially which will be revisited and re-adjusted to provide a fine trim of the aircraft with emphasis on cruise and on the critical stages of the flight which require the extension/retraction of the flaps (approach, base, final, and go-around).

4.2. Dynamic Modes Testing

4.2.1. Short Period

The short-term aircraft response characteristics are of paramount importance, since poor behavior can make the aircraft very difficult or even impossible for the pilot to handle, with catastrophic and even fatal consequences. As such, the primary goal when evaluating the flying and handling qualities of any design is to achieve a satisfactory short-term response, which is illustrated at the execution of the short period dynamic mode. The long-term response is also important, but the long period dynamic modes provide crucial time to the pilot to assess a potentially unstable aircraft behavior and make the appropriate handling decisions. The short period can be demonstrated by a sharp and short pull back, or push down, on the control column of a trimmed aircraft on steady level flight, releasing it, and measuring its response in relation to attitude of the aircraft. Due to the short term nature of the mode and to avoid potential inconsistencies of the recorded data, the trials of the mode on the engineering flight simulator were standardized by having two different persons executing the mode 10 times each, with instruction from a third person on the correct timing of the sharp and short control column input, after it has been verified that the aircraft was flying a trimmed, steady, and level flight. The short period mode has been tested by the test pilot as well. Through the data it was shown that the time period for the mode was an average of 3.5 seconds meaning a linear frequency of 0.286 s^{-1} and an angular frequency of 1.795 rad s^{-1} , which falls within the expected range of values, which is 1 rad/s to 10 rad/s [36]. The calculated value of the damping ratio suggests that the aircraft meets Level 2 safety until load force with respect to α (n/α) reaches 1.5. After this, it becomes Level 1, with the natural frequency of 2.268 rad/s and damping ratio of 0.611. According to MIL-F-8785C [37], the damping ratio of the short period meets all of the requirements for all the segments of the flight. Figure 10 shows a recording of an elevator impulse and Figure 11 the body axis pitch rate of a short period mode execution at cruise conditions.

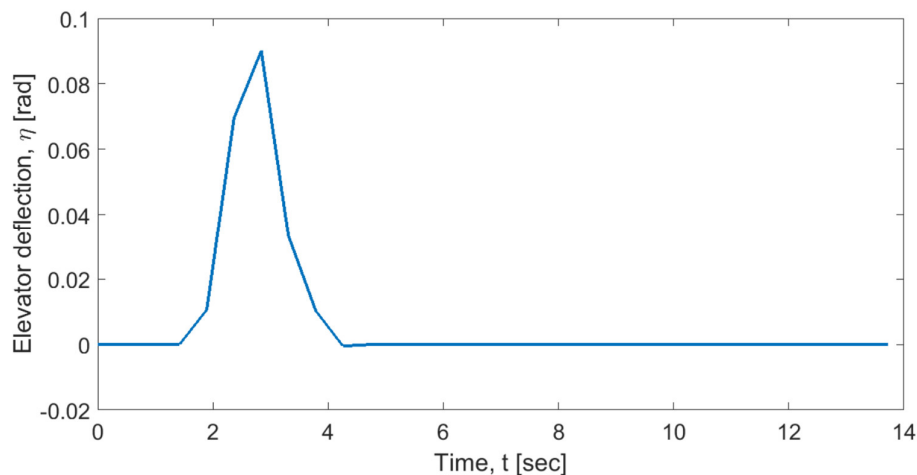
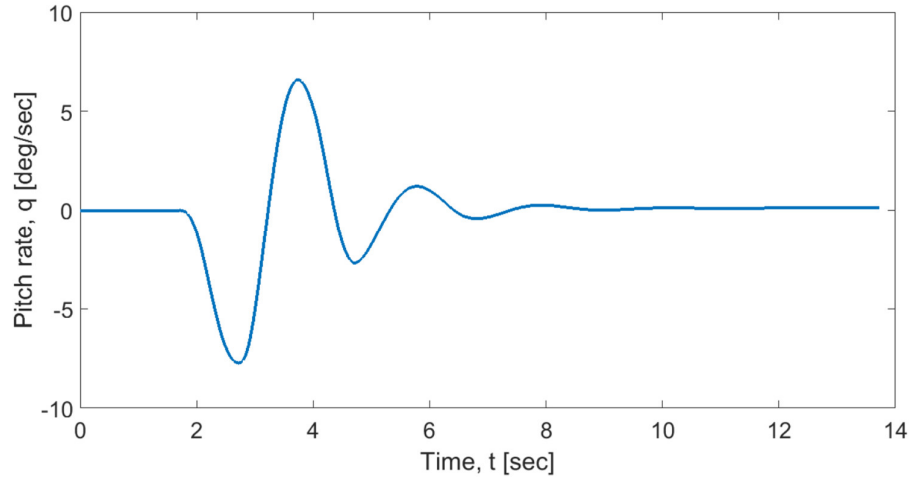


Figure 10. In flight elevator impulse input for short period mode at cruise conditions.**Figure 11.** In flight body axis pitch rate recording for short period mode at cruise conditions.

4.2.2. Long Period (Phugoid)

The phugoid can be initiated by pulling back (or pushing down), on the control column until 10% of the trim speed has been lost (or gained), then releasing it to determine its ability to return to the trimmed condition. Table 6 shows the related phugoid mode comparative results for two different trim airspeeds.

Table 6. Comparative results for the phugoid mode

| Speed (KIAS) | Simulated frequency (rad/s) | Theoretical frequency (rad/s) | % Difference |
|--------------|-----------------------------|-------------------------------|--------------|
| 347 | 0.0761 | 0.0776 | 2.47 |
| 507 | 0.0558 | 0.0532 | 4.77 |

The calculated damping was 0.180. In relation to the requirements of [37], the simulated response meets the requirements set out by the document with its minimum for level 1 flight being a damping ratio of at least 0.04.

4.2.3. Roll Subsidence (Roll Mode)

The mode is typically defined [40] as the “damping effects that normally oppose roll rate”; indicating the forces that are opposing an initiated aircraft roll. For the roll mode, [37] states that the requirements for category B flying is a roll mode time constant of 1.4 s or less, and category C flight to be less than or equal to 1.0 s. The maximum roll rate has occurred with $-11.53 \text{ deg s}^{-1}$. The result occurs at 36.8% of the value which is $-4.243 \text{ deg s}^{-1}$. The recorded data showed that this was achieved within 1.25 s, which is within the required range. The aircraft even returns above the negative roll rate to bring it back to its datum attitude.

4.2.4. Dutch Roll

The Dutch roll is the oscillation in yaw which is due to the change in velocity at each wing leading to roll [36]. The mode is initiated through a quick back-and-forth input of the right and left rudder pedals generating the oscillation. As part of the Dutch roll, the damping ratio for both category B and C phases of flight be greater than or equal to 0.08; while frequency for category B needs to be greater than or equal to 0.4 rad s^{-1} , but greater than or equal to 1.0 rad s^{-1} in category C. Natural frequency and damping ratio were calculated to be 2.512 rad s^{-1} and 0.552 respectively. These values meet the requirements of MIL-F-8785C [37], suggesting that the mode is satisfactory.

4.2.5. Spiral Mode

During the tests with a slow right rudder that would be released at 20° bank, the BWB aircraft would not go beyond 30°. However, if the pilot were to use the rudder adversely and expeditiously, the aircraft would respond dramatically rolling severely past 20° to 40° in under 2 seconds and continue rolling until it was 90° to the horizon, losing height rapidly. From this, it could be said that with sideslip perturbations, the aircraft would remain stable and safe. However, an excessive force such as that generated by the pilot in parallel with that of a large crosswind could put the aircraft in risk, particularly when at already low speeds like at the approach and landing phase. A design improvement, which resulted from the analysis of the spiral mode behavior, was to increase the size of the winglet rudders, a change that has enabled more control and resistance to external interference.

5. Conclusions

A series of studies that are cited at the present article have reported various technical challenges associated with the conceptual design and operation of the BWB aircraft. The challenges range from longitudinal and lateral instabilities to handling authority and weight efficiency. Some of those studies have suggested innovative remedies, such as winglet rudders, which enhanced the ability of BWB designs to perform various essential functions within satisfactory operational limits. At the same time, many of the proposed BWB designs of the literature have remained on their conceptual stage, without being further developed and tested on a large scale on a simulator, especially the designs which attempted to explore options for passenger capacity that are comparable to modern conventional passenger aircraft.

The present study has developed a baseline BWB design that offers a capacity of 200 passengers, the full scale of which has been flight tested at an engineering flight simulator. The adaptability provided by the functionality of the simulator has enabled the authors to implement design changes, and by carefully managing the configuration of the design, to apply design solutions which resulted in a BWB design that exhibits desired flying and handling qualities that satisfy typical existing certification requirements, which are applicable to conventional passenger jet configurations. Typical performance related trends observed at previous BWB conceptual design development studies in comparison to conventional passenger aircraft, such as higher L/D ratios, lower wing loading (W/S) values, and reduction of fuel required per mile to carry the same payload have been observed for the proposed BWB configuration as well. Amongst the novelties of the present study is that it has incorporated feedback that has been based on both test pilot inputs and actual analysis of flight simulation test data of the full size aircraft design, in addition to an achieved elliptical lift distribution. As such, a successfully designed concept for a BWB has been achieved which is statically stable with a confirmed dynamic stability flight behavior. The outcome of the study adds to existing insights about the controllability of a BWB configuration [41,42] and reinforces the outcomes of Karl and Wohlfahrt [8], that a BWB can be designed to be inherently stable.

As a future step, the study of the baseline BWB configuration can be further developed by applying high fidelity optimization techniques, the outcome of which can lead to further reshaping of the BWB configuration, including insights on the magnitude of the wave drag component of the design and how this can be minimized. This might subsequently allow the developed BWB design to achieve a higher than the already established maximum speed of 0.85 Mach.

Author Contributions: Conceptualization, I.L.; Data curation, C.H.-J., I.L., and D.M.S.; Formal analysis, C.H.-J. and I.L.; Investigation, C.H.-J., I.L., and D.M.S.; Methodology, C.H.-J. and I.L.; Project administration, I.L.; Resources, I.L.; Software, C.H.-J. and D.M.S.; Supervision, I.L.; Validation, C.H.-J., I.L., and D.M.S.; Visualization, C.H.-J., I.L., and D.M.S.; Writing – original draft, C.H.-J., I.L., and D.M.S.; Writing – review and editing, I.L. All authors have read and agreed to the published version of the manuscript.

Funding: This research received no external funding.

Acknowledgments: The authors would like to thank Georgios Makris for providing insightful ideas and suggestions.

Conflicts of Interest: The authors declare no conflicts of interest.

Acronyms

| | |
|------|---|
| AR | Aspect Ratio |
| BWB | Blended Wing Body |
| CDE | Computation Design Engine |
| ISA | International Standard Atmosphere |
| KIAS | Knots Indicated Air Speed |
| MAC | Mean Aerodynamic Chord |
| MOB | Multidisciplinary Optimization of a BWB |
| MTOW | Maximum Take Off Weight |
| NACA | National Advisory Committee for Aeronautics |
| OEW | Operating Empty Weight |
| RANS | Reynolds Averaged Navier Stokes |
| VLM | Vortex Lattice Method |

References

1. Liebeck, R. Design of the Blended Wing Body subsonic transport. *J. Aircr.* **2004**, *41*, 10–25.
2. Liebeck, R.; Page, M.A.; Rawdon, B.K. Blended Wing Body subsonic commercial transport. In Proceedings of the 36th AIAA Aerospace Sciences Meeting and Exhibit (AIAA-98-0438), Reno, NV, USA, 12–15 January 1998.
3. Liebeck, R.; Page, M.A.; Rawdon, B.K.; Scott, R.A. *Concepts for Advanced Subsonic Transports*; NASA CR-4624; NASA: Washington, DC, USA, 1994.
4. Okonkwo, P.; Smith, H. Review of evolving trends in Blended Wing Body aircraft design. *Prog. Aerosp. Sci.* **2016**, *82*, 1–23.
5. Wilkinson, K.; Shepperd, J.; Lyon, H. *The Longitudinal Response of Tailless Aircraft*; RAE Report 2060; Royal Aircraft Establishment: Farnborough, UK, 1945. Available online: <https://discovery.nationalarchives.gov.uk/details/r/C2428995> (accessed on 20 April 2020).
6. Rahman, N.U.; Whidborne, J.F. A lateral directional flight control system for the MOB Blended Wing Body planform. In Proceedings of the UKACC International Conference on Control, Manchester, UK, 2–4 September 2008.
7. Dubovikov, E.; Fomin, D.; Guseva, N.; Kondakov, I.; Kruchkov, E.; Mareskin, I.; Shanygin, A. Manufacturing aspects of creating low-curvature panels for prospective civil aircraft. *Aerospace* **2019**, *6*, 18.
8. Karl, N.; Wohlfahrt, M. *Tailless Aircraft in Theory and Practice*; AIAA Education Series: Washington, DC, USA, 1994; ISBN 978-1563470943.
9. Morris, A.; Arendsen, P.; La Rocca, G.; Laban, M.; Voss, R.; Honlinger, H. MOB-A European project on multidisciplinary design optimisation. In Proceedings of the 24th ICAS Congress, Yokohama, Japan, 29 August–3 September 2004.
10. Qin, N.; Vavalle, A.; Le Moigne, A.; Laban, M.; Hackett, K.; Weinerfelt, P. Aerodynamic considerations of Blended Wing Body aircraft. *Prog. Aerosp. Sci.* **2004**, *40*, 321–343.

11. Van Dommelen, J.; Vos, R. Conceptual design and analysis of Blended-Wing-Body aircraft. *Proc. Inst. Mech. Eng. Part G J. Aerosp. Eng.* **2014**, *228*, 2452–2474.
12. Risch, T.; Cosentino, G.; Regan, C.; Kisska, M.; Princen, N. X-48B flight test progress overview. In Proceedings of the 47th AIAA Aerospace Sciences Meeting including the New Horizons Forum and Aerospace Exposition, Orlando, FL, USA, 5–8 January 2009.
13. Potsdam, M.A.; Page, M.A.; Liebeck, R. Blended Wing Body analysis and design. In Proceedings of the 15th Applied Aerodynamics Conference (AIAA-97-2317), Atlanta, GA, USA, 23–25 June 1997.
14. Airbus Global Market Forecast-Growing Horizons 2019–2038. Available online: <https://www.airbus.com/aircraft/market/global-market-forecast.html> (accessed on 14 February 2020).
15. Boeing Commercial Market Outlook 2019–2038. Available online: <https://www.boeing.com/commercial/market/commercial-market-outlook/> (accessed on 14 February 2020).
16. Ammar, S.; Legros, C.; Trepanier, J.Y. Conceptual design, performance and stability analysis of a 200 passengers Blended Wing Body aircraft. *Aerosp. Sci. Technol.* **2017**, *71*, 325–336.
17. Mariens, J.; Elham, A.; van Tooren, M.J.L. Influence of weight modelling on the outcome of wing design using multidisciplinary design optimisation techniques. *Aeronaut. J.* **2013**, *117*, 871–895.
18. Roskam, J. *Airplane Design: Component Weight Estimation (Part V)*; DAR Corporation: Lawrence, KS, USA, 1999; ISBN 9781884885501.
19. Raymer, D. *Aircraft Design: A Conceptual Approach*; AIAA Education Series: Washington, DC, USA, 2012; ISBN 978-1-60086-911-2.
20. Torenbeek, E. *Advanced Aircraft Design, Conceptual Design, Analysis and Optimisation of Subsonic Civil Airplanes*; John Wiley and Sons Ltd.: West Sussex, UK, 2013; p. 410.
21. Boeing 737 Airplane Characteristics for Airport Planning. Available online: <https://www.boeing.com/resources/boeingdotcom/commercial/airports/acaps/737.pdf> (accessed on 4 April 2020).
22. Brandley, K.R. *A Sizing Methodology for the Conceptual Design of Blended Wing Body Transports*; Technical Report CR-213016; NASA Langley Research Center: Hampton, VA, USA, 2004.
23. Jenkinson, L.R.; Simpkin, P.; Rhodes, D. *Civil Jet Aircraft Design*; Butterworth-Heinemann: London, UK, 1999; ISBN 978-0340741528.
24. Siouris, S.; Qin, N. Study of the effects of wing sweep on the aerodynamic performance of a blended wing body aircraft. *Proc. Inst. Mech. Eng. Part G J. Aerosp. Eng.* **2007**, *221*, 47–55.
25. Dababneh, O.; Kipouros, T.; Whidborne, J.F. Application of an efficient gradient-based optimisation strategy for aircraft wing structures. *Aerospace* **2018**, *5*, 3.
26. McParlin, C.; Bruce, R.J.; Hepworth, A.G.; Rae, A.J. Low speed wind tunnel tests on the 1303 UCAV concept. In Proceedings of the 24th AIAA Applied Aerodynamics Conference (AIAA 2006-2985), San Francisco, CA, USA, 5–8 June 2006.
27. Lappas, I.; Ikenaga, A. Conceptual design and performance optimization of a tip device for a regional turboprop aircraft. *Aerospace* **2019**, *6*, 107.
28. Panagiotou, P.; Fotiadis-Karras, S.; Yakinthos, K. Conceptual design of a Blended Wing Body MALE UAV. *Aerosp. Sci. Technol.* **2018**, *73*, 32–47.
29. Jones, R.T. *The Spanwise Distribution of Lift for Minimum Induced Drag of Wings Having a Given Lift and a Given Bending Moment*; Technical Report TN-2249; NASA Ames Research Center: Mountain View, CA, USA, 1950.
30. Qin, N.; Vavalle, A.; Le Moigne, A. Spanwise lift distribution for Blended Wing Body aircraft. *J. Aircr.* **2005**, *42*, 343–356.
31. Kumar, P.; Khalid, A. Blended wing body propulsion system design. *Int. J. Aviat. Aeronaut. Aerosp.* **2017**, *4*, 1–43.
32. Qin, N.; Vavalle, A.; Le Moigne, A.L.; Hackett, K.; Weinerfelt, P. Aerodynamic studies for Blended Wing Body aircraft. In Proceedings of the 9th AIAA/ISSMO Symposium on Multidisciplinary Analysis and Optimization, Atlanta, GA, USA, 4–6 September 2002.
33. Da Ronch, A.; Drofelnik, J.; van Rooij, M.P.C.; Kok, J.C.; Panzeri, M.; Voß, A. Aerodynamic and aeroelastic uncertainty quantification of NATO STO AVT-251 unmanned combat aerial vehicle. *Aerosp. Sci. Technol.* **2019**, *91*, 627–639.

34. Merlin Flight Simulator Group Official Website. Available online: <http://www.merlinsim.com/mp521.htm> (accessed on 14 February 2020).
35. Merlin Flight Simulator Group. *MP521 Engineering Flight Simulator User Handbook*; TN8 6EJ; Kent, UK, 2017.
36. Cook, M.V. *Flight Dynamics Principles: A Linear Approach to Aircraft Stability and Control*, 3rd ed.; Butterworth-Heinemann: Amsterdam, The Netherlands, 2013; ISBN 9780080982427.
37. United States Department of Defense. *MIL-F-8785C 'Flying Qualities of Piloted Airplanes'*; United States Department of Defense: Arlington, VA, USA, 1980.
38. Etkin, B.; Reid, L.D. *Dynamics of Flight: Stability and Control*, 3rd ed.; Wiley: New York, NY, USA, 1995; ISBN 978-0-471-03418-6.
39. Nicolai, L.M.; Carichner, G. *Fundamentals of Aircraft and Airship Design: Aircraft Design Volume I*; American Institute of Aeronautics and Astronautics: Washington, DC, USA, 2010; ISBN 978-1-60086-751-4.
40. Stengel, R. *Flight Dynamics*; Princeton University Press: Princeton, NJ, USA, 2004; ISBN 978-0691114071.
41. Voskuil, M.; La Rocca, G.; Dircken, F. Controllability of Blended Wing Body aircraft. In Proceedings of the 26th ICAS Congress, Anchorage, AK, USA, 14–19 September 2008.
42. Cook, M.V.; de Castro, H.V. The longitudinal flying qualities of a Blended Wing Body civil transport aircraft. *Aeronaut. J.* **2004**, *108*, 75–84.



© 2020 by the authors. Licensee MDPI, Basel, Switzerland. This article is an open access article distributed under the terms and conditions of the Creative Commons Attribution (CC BY) license (<http://creativecommons.org/licenses/by/4.0/>).